



The effect of natural fractures on hydraulic fracturing propagation in coal seams



Tao Wang^{a,b,*}, Wanrui Hu^a, Derek Elsworth^c, Wei Zhou^a, Weibo Zhou^d, Xianyu Zhao^a, Lianzheng Zhao^a

^a State Key Laboratory of Water Resources and Hydropower Engineering Science, Wuhan University, China

^b State Key Laboratory of Coal Resources and Safe Mining, China University of Mining and Technology, Beijing, China

^c Department of Energy and Mineral Engineering, G3 Center and EMS Energy Institute, Penn State University, University Park, PA, USA

^d Northwest Engineering Corporation Limited, Power China, Xi'an, China

ARTICLE INFO

Keywords:

Hydraulic fracturing
Particle flow method
Natural fracture
Coal seam

ABSTRACT

The purpose of hydraulic fracturing is to improve the gas permeability of a coal seam by the high-pressure injection of fracturing fluid into cracks. Some promising results of hydraulic fracturing in a coal seam using isotropic and intact model have been published in our previous study (Wang et al., 2014), based on which further research is necessary for the reason that natural coal is anisotropic, inhomogeneous, inelastic, and characterized by multiple discontinuities, which can be one of the most important factors governing the deformability, strength and permeability. It is difficult to accurately identify and predict the manner in which hydraulic fractures initiate and propagate because of the pre-existing natural fractures. In this paper, five typical coal models—intact coal, layered jointed coal, vertical jointed coal, orthogonal jointed coal, and synthetic jointed coal—are established to simulate hydraulic fracturing in coal seam based on two-dimensional particle flow code (PFC2D). The effect of natural existing fractures on fluid-driven hydraulic fracture is investigated by analyzing the variation of fracture radius, cumulative crack number, and growth rate of porosity versus injection time. It is shown that the existence of natural fractures, which has a significant induced effect on the initiation and propagation of hydraulic fracture, contributes greatly to the increase of crack number and growth rate of porosity. The fracture network is greatly influenced by the interaction between hydraulic fracture and natural fractures. Natural fractures with different structural properties may result in different propagation types of hydraulic fracture, which can be categorized as capturing type, crossing type, and compound type.

1. Introduction

Today, Hydraulic fracturing (HF) is used extensively in the petroleum industry to stimulate oil and gas wells to increase their productivity (Adachi et al., 2007). Cipolla and Wright (2000) detailed the state of the art in applying both conventional and advanced technologies to better understand HF and to improve treatment designs. The permeability of coal-bed methane reservoirs in China is so low that it must be stimulated before the gas can be produced (Wright et al., 1995; Shan et al., 2005; Li et al., 2010). Research efforts in recent year have proved that the hydraulic fracturing technology, adopted as an efficient stimulation approach, can significantly enhance the coal seam permeability, thus improving the productivity of coal-bed methane (Yuan et al., 2012; Hou et al., 2013; Li et al., 2014). Coal seams are dual porosity reservoirs that consist of porous matrix and cleat (fracture) network. During the process of hydraulic fracturing,

high-pressure fluid penetrates into both the matrix and the cleats along many artificially induced cracks, which not only extrude and release gas, but also provide transportable passage for gas. However, it is difficult to control or predict the effects of hydraulic fracturing because of geologic complexity and mechanism uncertainties. Wu et al. (2006) have found hydraulic fractures mainly have three kinds of mode in coal seams in China: predominantly horizontal fracture system; priority with vertical fracture system and complex fracture system, but the forming mechanism of different hydraulic fracture modes has not been well understood.

During the past six decades, considerable effort has been applied to understand the mechanics of hydraulic fractures (Chang, 2004). The Finite Element Method (FEM) and the Boundary Element Method (BEM) have been used to simulate HF in complex structures (Papanastasiou, 1997; Vychytil and Horii, 1998). Wang et al. (2010) have proposed a coupled algorithm combining FEM and a meshless

* Corresponding author at: State Key Laboratory of Water Resources and Hydropower Engineering Science, Wuhan University, China.
E-mail address: htwang@whu.edu.cn (T. Wang).

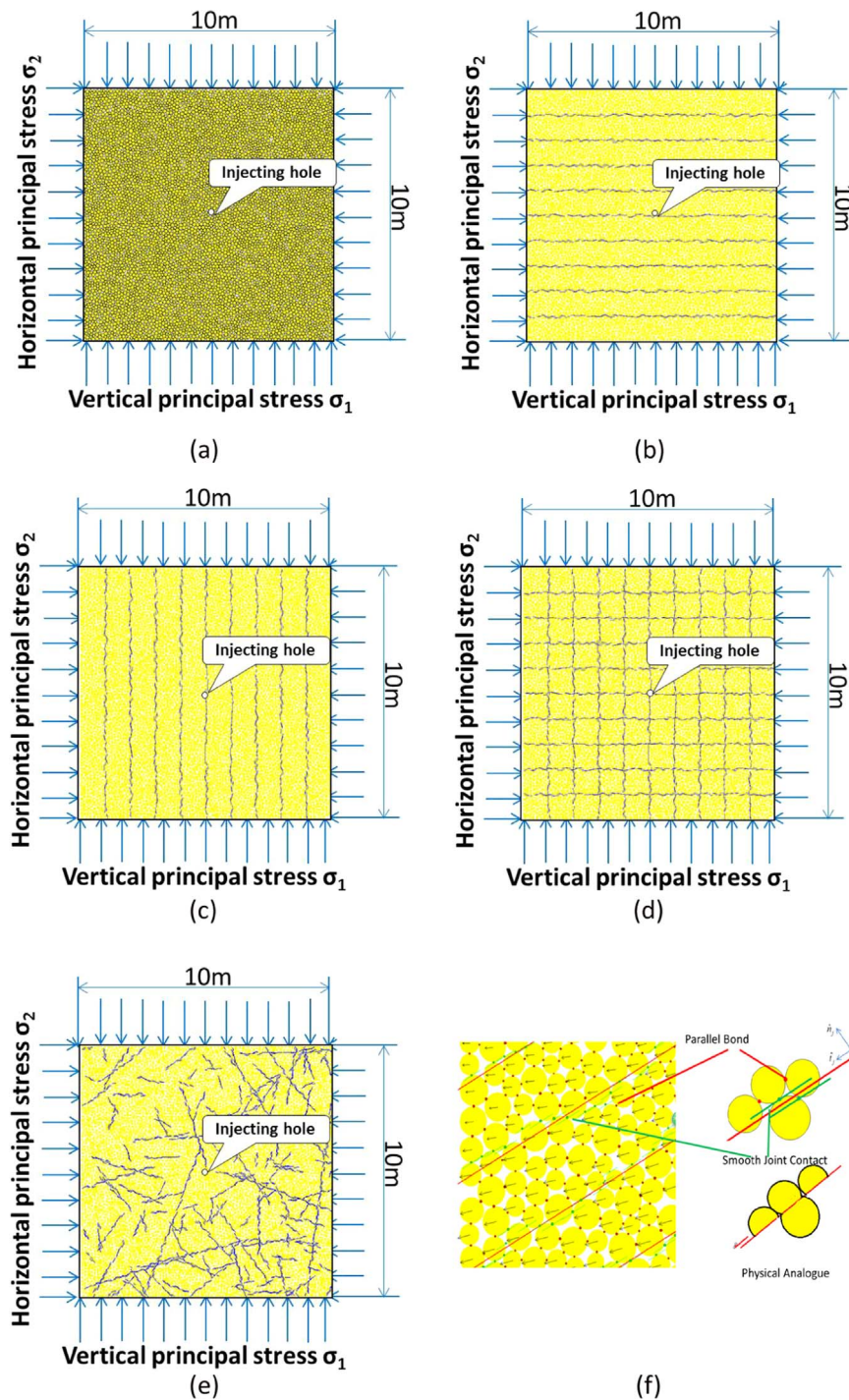


Fig. 1. HF calculation models of different types of coal rock mass: (a) intact coal model; (b) layered jointed coal model with a series of horizontal joints; (c) vertical coal model with a series of vertical joints; (d) fractured coal with a series of orthogonal joints and rock blocks; (e) synthetic jointed coal model in which a discrete fracture network is generated; (f) Concept of smooth joint contact model.

method for the simulation of the propagation of fracturing under either external forces or hydraulic pressure. In attempts to validate the models, microseismic monitoring has been used to image the extent and nature of hydraulic fractures. One of the major findings of these studies is that the nature of the hydraulic fractures determined by observing the recorded seismicity does not generally agree with that predicted by conventional analytical and numerical models (Al-Busaidi et al., 2005). For this reason discontinuum-based discrete element methods (DEM) have been applied to the simulation of HF. With these techniques, the continuum is divided into distinct blocks or particles between which fluid can flow. This allows for a better understanding of

hydraulic fracture growth in the coal rock mass, which may contain multiple pre-existing cracks, joints or flaws. The particle flow DEM has become an effective tool for modeling crack propagation (Potyondy and Cundall, 2004; Li et al., 2016). Al-Busaidi et al. (2005) simulated HF in granite using DEM with the results compared to acoustic emission data from experiments. The propagation of HF in coal seams under high-pressure water has been simulated using RFPA based on the maximum tensile strain criterion (Du, 2008; Huang, 2009). Shimizu (2010) and Shimizu et al. (2011) performed a series of HF simulations in competent rock using a coupled flow-deformation DEM code to investigate the influence of fluid viscosity and particle size distribution.

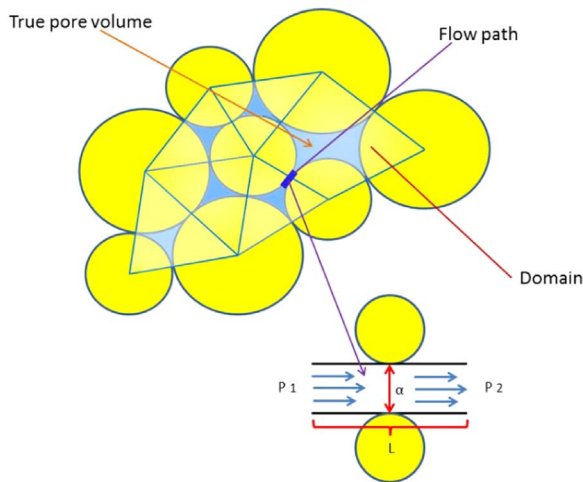


Fig. 2. Flow model in a bonded assembly of particles (Wang et al., 2014).

McLennan et al. (2010) described an approach to representing and assessing complex fracture growth and associated production prediction through generated fractures using DEM. Wang et al. (2014) used PFC^{2D} to simulate HF propagation within a coal seam. The objectives of the work were to investigate the trends governing crack propagation in a coal seam, propose schemes that could achieve the desired fracturing effects, and aid in optimally guiding engineering practices. However, the literature have mainly focused on HF propagation in intact rock; currently, simulation of HF in jointed rock masses is insufficient although the existence of natural fracture network is believed to be one of the main factors influencing the initiation and propagation of hydraulic fracture (Fan et al., 2014). From mine-back experiments and laboratory tests, Warpinski and Teufel (1987) noted that geologic discontinuities such as joints, faults, and bedding planes can significantly affect the overall geometry of the resulting hydraulic fractures. This can occur by arresting the growth of the fracture, increasing fluid leakoff, hindering proppant transport, and enhancing the creation of multiple fractures. Han et al. (2012) presented a microscopic numerical system to model the interaction between HF and natural fractures. Grasselli et al. (2014) presented preliminary results obtained using combined finite-discrete element techniques to study the interaction between fluid driven fractures and natural rock mass discontinuities. Zhang et al. (2014) using a hybrid discrete-continuum numerical model to simulate HF crossing and interaction with natural fractures or weakness planes in naturally fractures reservoir system. In this paper, based on our previous work of hydraulic fracturing in intact coal seam (Wang et al., 2014), we use a particle flow DEM to simulate and analyze the characteristics of HF propagation in coal rock masses with five different structures to reveal the effects of natural fractures on the initiation propagation influences of natural fractures.

2. Coal rock mass models for hydraulic fracturing

2.1. Selected models

Five typical coal models are selected as representative in this study. These represent intact, layered and jointed, vertical-jointed, orthogonal-jointed and then synthetic rock mass (SRM) of coal models. These conceptual models are used for the numerical simulation of HF using the two-dimensional particle discrete element program (PFC^{2D}). The study focuses on the initiation then propagation of HFs as affected by natural fractures.

The size of the models is 10 m×10 m. The particle radius R in the model ranges from R_{\min} (minimum of particle radius) to R_{\max} (maximum of particle radius) with a uniform distribution. The minimum radius of the particles is 0.05 m, the ratio of the maximum to

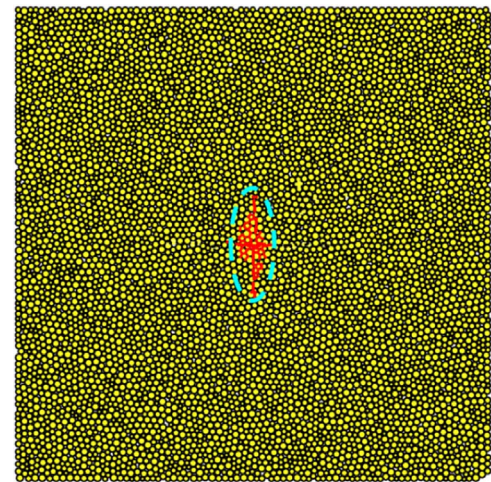


Fig. 3. Schematic description of fracture radius measured adjacent to the HF (red lines indicate broken bonds between particles). (For interpretation of the references to color in this figure legend, the reader is referred to the web version of this article.)

the minimum radius of the particles is 1.66, and 6622 particles are generated for the square model. The square-filling particle assembly is enclosed by four servo-controlled walls allowing initial stresses to be imposed. Five calculation models are constructed, as illustrated in Fig. 1. In all models, described above, the intact coal is represented by the bonded particle model (BPM), and pre-existing natural fractures are simulated by the smooth-joint model (SJM) (Itasca, 2010). The smooth-joint model was first proposed to model the presence of joints in fractured rock masses. The smooth joint model simulates the behavior of an interface, regardless of the local particle contact orientation along the interface. As shown in Fig. 1(f), the behavior of a joint can be modeled by assigning smooth joint models to all contacts between particles that lie on the opposite side of the joint (Wang et al., 2016).

It seems evident that DEM is a suitable approach for modeling the solid matrix component. In these investigations, different fluid flow methods (e.g., LBM (Han and Cundall, 2013), SPH (Robinson et al., 2014), DNS (Gui et al., 2010), pipe network (Han et al., 2012), etc.) were employed to simulate the effects of the fluid flow in the pore space. In a PFC model, a pipe network model is adopted to simulate the fluid flow between particles. The pipes between particles normally can be simplified as a pair of smooth, parallel plates. Therefore, the well-known “cubic law” can be applied to describe the fluid flow in fractures. The fluid “domain” and fluid “pipe” are adopted to numerically simulate the fluid-mechanical coupling (Wang et al., 2014). The initial pore water pressure is applied in all “domains” of the generated models to simulate the effect of groundwater in the rock mass. The initiation, opening and extension of HF are monitored via fluid-mechanical coupling by continuously applying fluid pressure in the center of the models.

2.2. Fluid flow through contacts and fluid mechanical interaction

The fluid flow in the pipe is assumed to obey Poiseuille channel flow (Fig. 2):

$$q = -\frac{a^3}{12\mu} \frac{(p_2 - p_1)}{l} \quad (1)$$

where l is the pipe length, which is assumed to be the sum of the radii of two particles; p_2 and p_1 are pressures inside the two connected domains (inlet and outlet); μ is the fluid viscosity; and a is the hydraulic aperture of the contact, which varies with model geometry and deformation.

The simple relationship below ensures that aperture a approaches

Table 1
Microscopic parameters of BPM and SJM and calibrated macro characteristic parameters.

Microscopic parameters of BPM and SJM					
BPM		SJM			
R_{min} /m	0.05	\bar{k}_n /GPa/m	70		
R_{max}/R_{min}	1.66	\bar{k}_s /GPa/m	70		
ρ /kg/m ³	1635	$\bar{\lambda}$	1.0		
μ	0.7	μ	0.5		
E_c /GPa	5.0	ψ /°	10		
k_n/k_s	2.5	M	3		
$\bar{\lambda}_{pb}$	1.0	σ_c /MPa	7.0		
\bar{E}_c /GPa	5.0	c_b /MPa	7.0		
$\bar{\sigma}_c$ /MPa	15	ϕ_b /°	0		
$\bar{\tau}_c$ /MPa	15	Porosity	0.15		
\bar{k}^n/\bar{k}^s	2.5				
Calibrated macro-mechanical parameters of different coal rock masses					
	Intact	Layered	Vertical jointed	Orthogonal jointed	Synthetic jointed
UCS/MPa	14.25	11.96	11.34	9.00	7.06
Elasticity modulus /GPa	3.22	2.92	2.85	0.51	0.59

Table 2
In situ stress and injection parameters.

Parameters	Value
Vertical principal stress MPa	12
Horizontal principal stress MPa	6
Injection time s	100
Injection flow rate m ² /s	1.0e-3
Initial pore pressure MPa	1.0
Injected fluid Viscosity Pa s	0.01

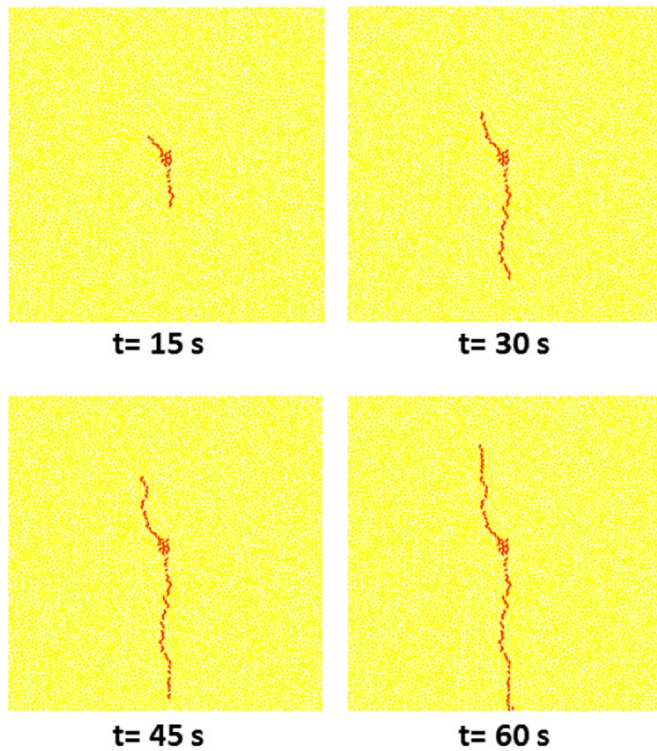


Fig. 4. The propagation and distribution of HF cracks in an intact coal.

zero-force aperture for zero normal-contact force and converges toward zero for an extremely large normal-contact force:

$$a = \frac{a_0 F_0^n}{F^n + F_0^n} \quad (2)$$

where F^n is the normal contact force; F_0^n is the normal contact force at which the aperture a equals $a_0/2$; and a_0 is the zero-force aperture.

The coupling of fluid pressure with volumetric deformation is resolved within the granular domain. The deformation of particles surrounding a domain change its volume and adjust the fluid pressure of the domain. Resulting flows into the domain may similarly induce changes in pressure. Therefore, full hydro-mechanical coupling is considered when new cracks form in the model (via bond breakages); these are automatically connected to the existing pipe network. In this manner, it is possible to simulate the evolution of fracture volume changes and network connectivity as a result of fluid injection.

2.3. Generation of discrete fracture network

PFC^{2D} has been successfully used to study the mechanical behavior of discrete fracture network (DFN) systems via a smooth-joint contact model (Mas Ivars et al., 2008). The modeling approach consists of superimposing fracture information (i.e., fracture geometries and properties) onto a bonded-particle model (BPM) (Potyondy, 2012). The BPM is used to model intact rock, and the mechanical behavior of the fractures is introduced by modifying the contact models at contacts intercepting the fractures. Because PFC models are inherently discrete, failure can occur both in the intact BPM regions and along the fracture planes. The determination of rock mass properties from such a configuration has been termed SRM methodology.

Within the DFN module, the fracture group embedded into the rock mass is viewed as a set of discrete, planar and finite-sized fractures. The DFN modeling approach is stochastic; the geometrical characteristics of the DFN model are constrained only by the independent statistical distributions (type of distribution and associated parameters) of its geometrical properties. The geometrical characteristics currently supported by the DFN module are the distributions of fracture size, orientation and position. From one (stochastic) DFN model, any number of different DFN realizations can be generated, depending on a random seed. The validation of DFN results relies on the collection of objects describing the fractures and associated properties.

3. Parametric selection

The injection borehole for the generation of the HF is located in the center of the model (Fig. 3). The initial pore pressure is first applied, and then the injection pressure is increased continually by constant flow injection until breakdown of the borehole occurs and a fracture is initiated. Parameters associated with the BPM and SJM (Mas Ivars et al., 2008) are specified before simulation of HF via a numerical

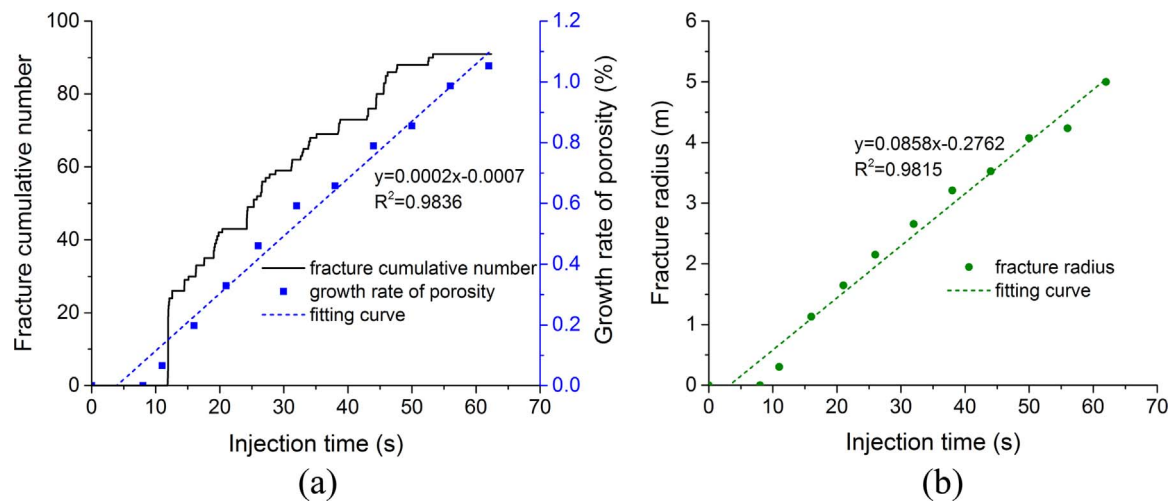


Fig. 5. Simulated results of intact rock mass: (a) development of fracture cumulative number and growth rate of porosity versus injection time; (b) propagation of fracture radius versus injection time.

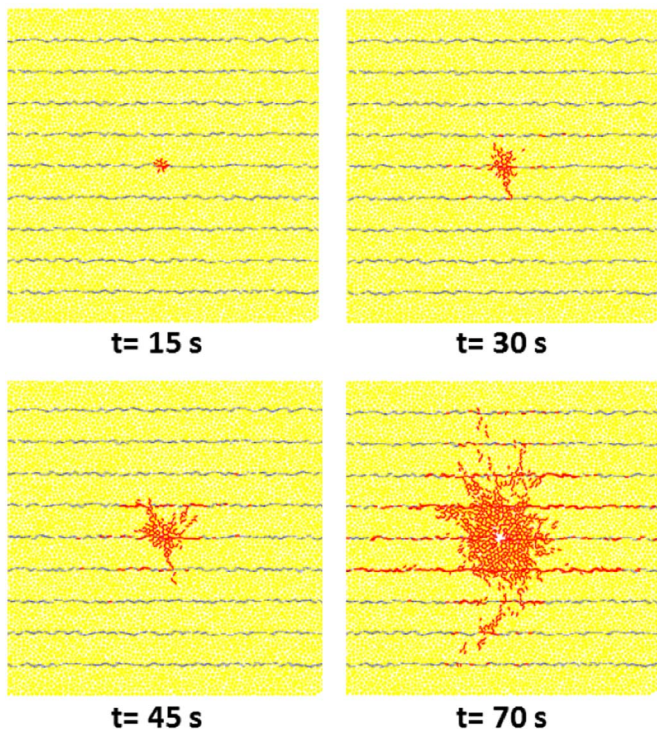


Fig. 6. Propagation and distribution of HF cracks in layered jointed coal.

compression test conducted by constantly adjusting microscopic parameters to bring the macroscopic parameters of the model close to the mechanical characteristic parameters that are observed in experiments. On the basis of prior research results (Wang et al., 2014) on the corresponding quantitative relationships between macroscopic and microscopic parameters of particle discrete elements, a series of uniaxial compression tests are performed to select proper microscopic mechanical parameters. Microscopic and macroscopic parameters (based on field mechanical tests of coal in Yuyang Coal Mine in China) of the model after specific calibration, in situ stress, and injection parameters selected are shown in Tables 1, 2.

4. Numerical simulation results

Five types of typical coal rock mass models are established to conduct numerical calculations, and fracture distribution and cumula-

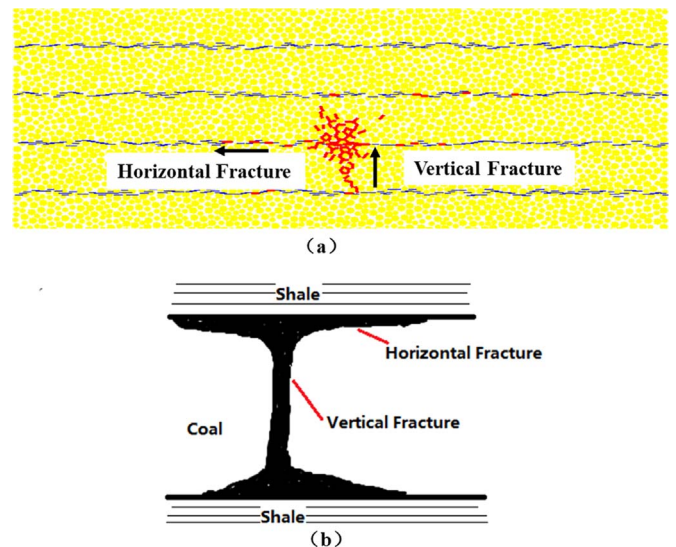


Fig. 7. Simulated and in-field vertical and horizontal fractures: (a) Simulation graph of partial enlargement; (b) Horizontal and vertical fractures formed after HF treatment in field, modified from Wu et al. (2006).

tive numbers of fractures are recorded as they evolve with time. Moreover, the fracture radius is obtained by measuring semi major axis length of the ellipse (Fig. 3) that envelops all the developed fractures near the injection hole. Thus, the evolution of crack initiation and propagation can be observed and codified in both time and in space. The BPM simulates the behavior of a set of particles connected by a bond, and their microcracks are represented explicitly as broken bonds, which form and coalesce into macroscopic fractures when a load is applied (Camones et al., 2013). Many references (Li and Wong, 2012; Duan and Kwok, 2015) have proved that the coalescence of microcracks and macroscopic fractures have a good consistence. Through crack extension and opening the porosity of the particle assembly increases, so the evolution of coal permeability may be indirectly characterized by calculating the growth rate in porosity of the particle assembly adjacent to the injection hole.

4.1. HF propagation in intact coal

The crack propagation and evolution of the HF for the intact coal without joints is as shown in Fig. 4. A relatively complete continuous vertical fracture develops without bifurcation is eventually formed

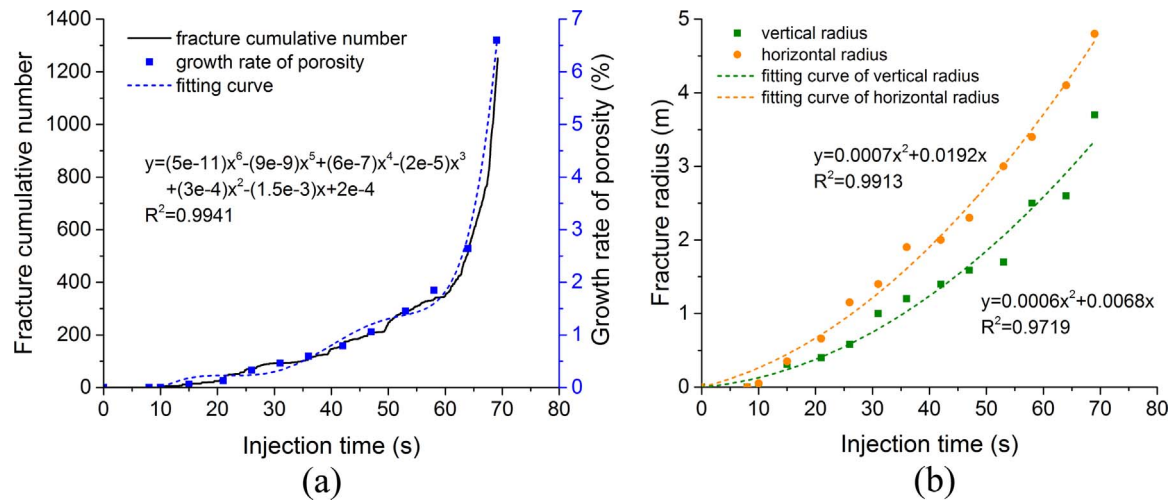


Fig. 8. Simulated results of layered jointed coal: (a) development of fracture cumulative number and growth rate of porosity versus injection time; (b) propagation of fracture radius versus injection time.

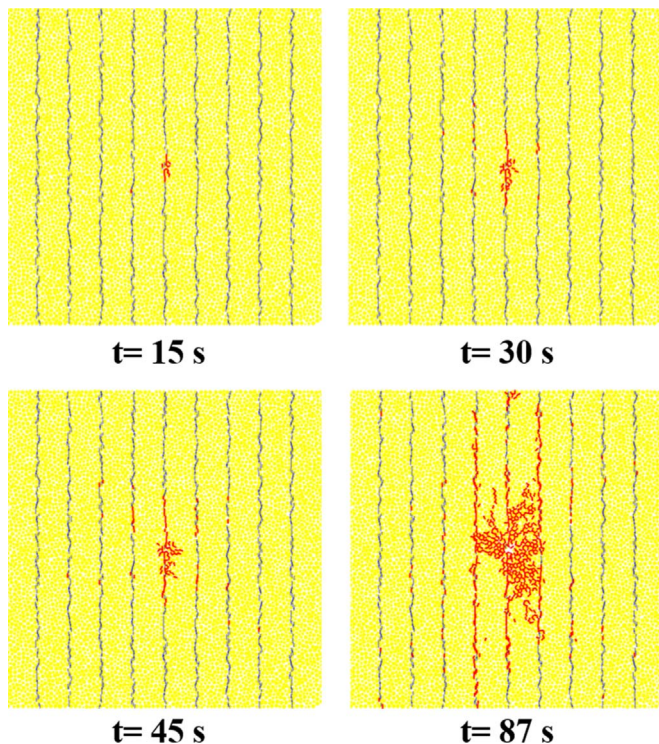


Fig. 9. Propagation and distribution of HF cracks in the vertical jointed coal.

consistent with the in situ stress conditions that are applied (the maximum principal stress is in the vertical direction).

As shown in Fig. 5, the development of the fracture can be observed from the curve representing the cumulative number of cracks (broken bonds) that develop with time in the intact coal. The hydraulic pressure is initially too low to fracture the rock at the initiation of pressurization. The cracks that develop around the borehole coalesce and extend in the vertical direction at time $t=12$ s. A single continuous crack propagates later at time $t=30$ s. In the meantime, the cumulative number of fractures develop along a linear trajectory, and the crack propagates along the direction parallel to the vertical principal stress. It is not until time $t=60$ s that the crack crosses through the whole model. The numerical simulation results of HF in the intact rock mass agree with the physical results of most HF tests and the laws reflected in the classical theory of elastic mechanics (Hubbert and Willis, 1957; Wang and Tonon, 2009). The fracture radius (Fig. 5(b)) and growth rate of

porosity (Fig. 5(a)) around the injection hole present a linear increase since the crack propagates to termination evenly without bifurcating.

4.2. HF propagation in layered jointed coal

Layered jointed coal is formed in the long process of geological deposition and folding. Therefore, their strength and deformation have typically anisotropic characteristics. In this section, a two-dimensional layered coal model is constructed with horizontal joints running across the entire model with a joint spacing of 1 m. The propagation and distribution of a hydraulic fracture in such a jointed coal under the applied conditions is presented in Fig. 6.

Initial fractures are mainly distributed around the injection hole as pressurization begins and propagate from this source in all directions; however, a complete continuous crack similar to the simulation result of intact coal does not appear. The main reason for this result is that a pre-existing joint surface passes near the injection hole, which runs through the whole model and forms a complete crack channel that acts as a “tributary” and disperses the flow near the injection hole. Thus, the flow in the vertical direction is sharply decreased, and the induced pore pressure is accordingly decreased. Under these conditions it is difficult to form a comparatively complete crack with a clear propagation orientation in this direction. In the initial stage of injection, cracks mainly initiate and propagate along the horizontal joint surface and around the injection hole.

At time $t=30$ s, the two joints nearest the injection hole are almost connected by the vertical fractures, and thus an “I” or “T” type crack similar to the hydraulic fractures observed in shale and coal seams forms (Fig. 7). The two connected joint surfaces constantly stretch, and the horizontal cracks continuously extend outward under the action of fluid pressure; simultaneously, the vertical cracks slowly extend outward. At time $t=70$ s, the horizontal cracks form on almost all joint surfaces with the longest horizontal crack throughout the entire model and coal near the injection hole fully fractured into dense cracks.

It can be seen from the cumulative crack number-vs-time curve (Fig. 8(a)) that the number of fractures increases linearly in the initial stage and then rapidly increases owing to the connection of more joints and the simultaneous rapid propagation of horizontal cracks. Then, the number of cracks sharply increases at time $t=60$ s; at that moment, the model has already approached a predominantly damaged state. As shown in Fig. 8(b), both the vertical and horizontal fracture radii quadratically increase with the injection time while the horizontal fracture propagates faster than the vertical fracture. Owing to the clearly layered interfaces in the horizontal direction and weak bond strength in these interfaces, it is easy to fracture the interface and thus

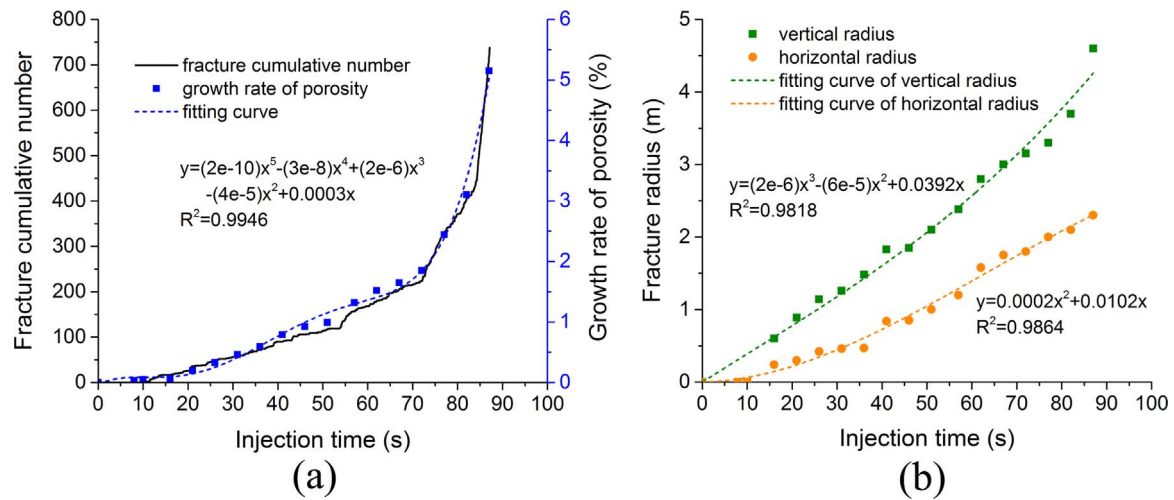


Fig. 10. Simulated results of vertical jointed coal: (a) development of fracture cumulative number and growth rate of porosity versus injection time; (b) propagation of fracture radius versus injection time.

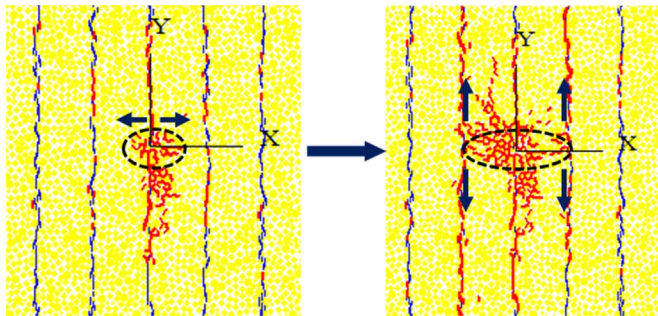


Fig. 11. Partial enlargement in the process of horizontal cracks developing into vertical cracks.

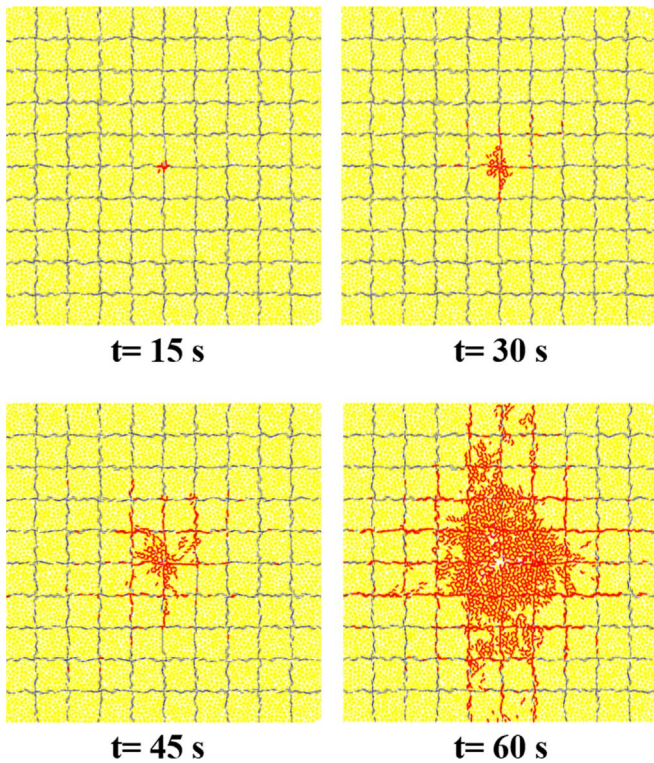


Fig. 12. Propagation and distribution of HF cracks in orthogonal jointed coal.

cause the cracks to propagate along the horizontal direction. Moreover, it is difficult for the cracks to break through the coal on either side of the interfaces to propagate outward. With the continuous emergence of cracks, the growth rate of porosity around the injection hole has been greatly improved compared to the intact coal in a variation law identical to the cumulative crack number-time curve (Fig. 8(a)). Thus, for the coal with distinct stratification characteristics, the characteristics of discontinuities play a crucial role in the propagation and spatial distribution of cracks, which may also be affected by the in situ stress.

4.3. HF propagation in a vertical jointed coal

We construct a simplified two-dimensional vertical jointed coal model for HF calculation; the simulation of crack propagation and distribution patterns is shown in Fig. 9.

As shown in Fig. 9, at time $t=10$ s, the model begins to crack, and cracks begin to slowly extend. At time $t=15$ s, it can be seen that a continuous vertical crack has formed along the joint in the middle of the model. Under the fluid pressure, the cracks continue to open along the joint, continuously extending from the center to the sides and downward, and the horizontal crack extends very slowly around the hole. However, it can be seen from the crack distribution when time $t=30$ s and 45 s that sporadic cracks are also distributed on the two joint surfaces near the center. The main reason is that the maximum principal stress of the model is applied in the vertical direction, and that the joint surface with the lower adhesive strength is also distributed along the vertical direction, which is close to the center of the injection holes. Tension failure cracks may occur in the coal under the interaction of initial stress and fluid pressure.

As shown in Fig. 10(a), in the process of crack propagation in HF, the cumulative number of cracks shows the regularity of substantially linear increases at time $t=55$ s. It shows rapid growth during the period of 55–80 s, mainly because the horizontal cracks near the center develop in vertical direction, and vertical joint planes are connected and quickly extend toward both ends. Especially before the vertical cracks cross through the whole model, the cumulative number of cracks surges.

As shown in Fig. 10(b), both the vertical and horizontal fracture radii quadratically increase with the injection time while the horizontal fracture propagates faster than the vertical fracture. Owing to the clearly layered interfaces in the horizontal direction and weak bond strength in these interfaces, it is easy to fracture the interface and thus cause the cracks to propagate along the horizontal direction. Moreover, it is difficult for the cracks to break through the coal on either side of

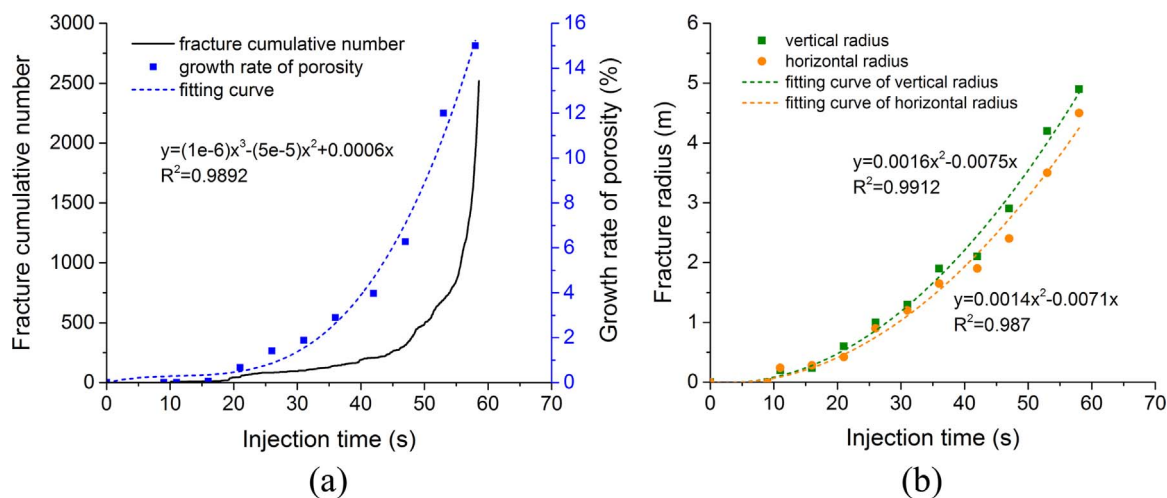


Fig. 13. Simulated results of orthogonal jointed coal: (a) development of fracture cumulative number and growth rate of porosity versus injection time; (b) propagation of fracture radius versus injection time.

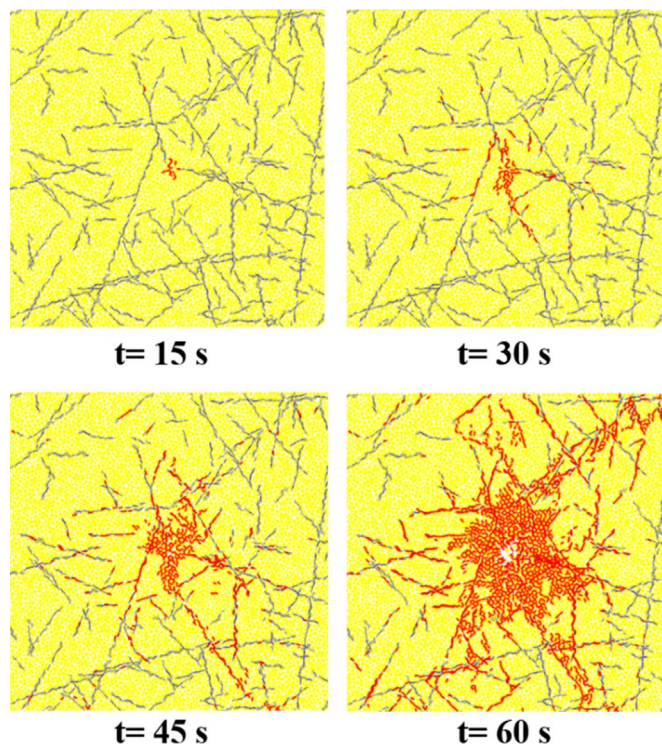


Fig. 14. Propagation and distribution of HF cracks in SRM.

the interfaces to propagate outward. With the continuous emergence of cracks, the growth rate of porosity around the injection hole has been improved compared to the intact coal in a variation law identical to the cumulative crack number-time curve (Fig. 10(a)). Thus, for the coal with distinct stratification characteristics, the characteristics of discontinuities play a crucial role in the propagation and spatial distribution of cracks, which may also be affected by the in situ stress.

With the continuous injection of fluid, coal near the injection hole is constantly being crushed and gathers a large number of cracks; when the horizontal cracks near the injection hole extend to two joint surfaces closest to the center joint surface, the joint surfaces will guide its propagation along the surface, and horizontal cracks will thus develop along vertical direction (Fig. 11). After the calculation, cracks generated by HF present a distribution similar to a narrow belt shape. Therefore, for vertical jointed coal, the generation and distribution of cracks in HF is affected mainly by discontinuities.

4.4. HF propagation in an orthogonally jointed coal

Coal with orthogonal fractures is another simplification. Thus, a series of simplified orthogonal joints is adopted to cut the rock and form a fractured structure, the model shown in Fig. 12 is constructed by using a series of orthogonal SJM models in the intact coal model.

It can be seen from the results of the fracture distribution calculation that fractures mainly generate and extend along the horizontal and vertical joints near the injection point in the initial stage (Fig. 12, at time $t=15$ s). At time $t=30$ s, the horizontal and vertical joints near the injection hole form a full continuous crack “template at 90 degrees” and with the continuous injection of fluid, the number of cracks increases, and the existence of the joint plays a key role of guiding the formation of HF cracks. Meanwhile, under the action of fluid pressure, the cracks develop toward both sides of the joint surface, and the rock blocks on both sides begin to crack. At time $t=45$ s, many cracks are generated near the injection hole, and three continuous cracks are formed along the horizontal and vertical directions. At that moment, under the action of fluid pressure, the number of cracks increases rapidly. Cracks near the injection hole continuously develop in the radial direction and along the nearby joints; these cracks generally present a symmetric extension. At time $t=60$ s, it can be seen that in the center of the whole model, the fractures are relatively symmetrical and a complete fracturing zone develops, with the cracks distributed continuously along the injection hole and along the horizontal and vertical joints. The cracks along the joint surfaces near the center traverse the model, and the cracked zone width decreases progressively from the center to the ends, generally presenting a rhombic distribution.

It can be seen from the curve of fracture radius versus time (Fig. 13(b)) that the vertical and horizontal fracture radii of the whole model basically accord with the quadratic growth law, and the growth rate of horizontal cracks is basically the same as the vertical cracks; this is mainly because cracks in the horizontal and vertical direction present a type of symmetric extension. With the continuous opening and extending of cracks in the fracturing process, the growth rate of porosity surrounding the injection hole has improved and increased cubically (Fig. 13(a)). The growth rate of the final porosity is approximately 16%, which is greatly enhanced compared to that of the foregoing three models, mainly because the model with more regular joints is more conducive to the extension of cracks.

4.5. HF propagation in a synthetic jointed coal

As previously described, the structural planes of the coal model are

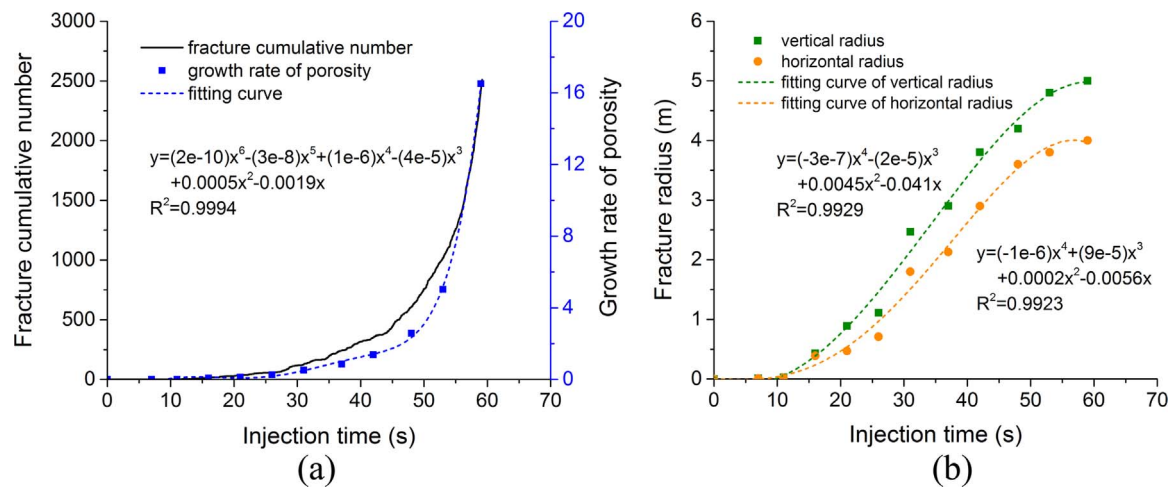


Fig. 15. Simulated results of SRM: (a) development of fracture cumulative number and growth rate of porosity versus injection time; (b) propagation of fracture radius versus injection time.

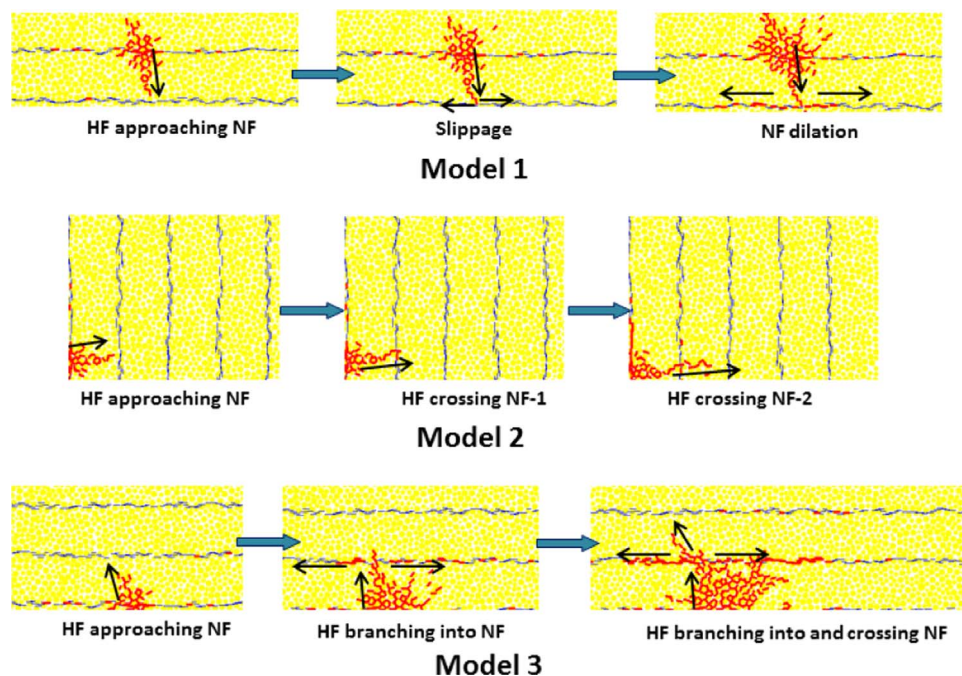


Fig. 16. Three patterns of the effect of natural fractures on the propagation of hydraulic fractures.

relatively simple, and they have obvious stratification and structural features. A coal rock mass has a distributed structure with randomly distributed and discontinuous structural planes that are different in size, dip angle and dip direction. This gives the rock mass scale-dependent structural properties. The spatial interaction of discontinuous structural planes forms a network of complex fractures such that the rock mass becomes a non-uniform and discontinuous structure with more complex and scale dependent deformation and strength properties. DFNs have become an effective method to study the characteristics of fractured rock masses (Mas Ivars et al., 2011; Pierce and Fairhurst, 2012). Here we use DFN technology to generate a fracture network and add these fractures to the intact rock mass. Similarly, the intact rock mass uses BPM, and the random fracture uses SJM; thus, the SRM can be constructed to reflect the characteristics of fractured rock mass.

The SRM technique is used to simulate jointed coal to research HF propagation, and the distribution of the cracks is finally obtained (Fig. 14). At the beginning of HF stimulation, the coal around the injection hole is relatively intact, and no joint passes through the

injection hole. Thus, the fractures are mainly caused by the rupture of the intact coal, and the cracks mainly extend in the vertical direction. At time $t=15$ s, the upper end of the vertical crack basically connects with the nearest natural fracture. When the hydraulic fractures and the natural fractures are connected, all cracks essentially develop along the natural fracture. As shown in Fig. 14, several cracks near the injection hole connect and form multiple continuous fractures. At the same time, the intact coal near the injection hole is continuously cracked under the sustained action of the high-pressure fluid, and more random cracks are penetrated. The fluid flows along each crack, and the cracks continue to spread and expand under the effect of the fluid wedge. Finally, there is a large fractured zone around the center of the model at time $t=60$ s, and the complex HF network in which cracks intertwine and bifurcate everywhere is formed. It can be seen from the curve of fracture radius versus time in Fig. 15 that the variation rule is similar to the previous models, the growth rate of the crack increases with time, and the crack number grows steep rise when it is near the point of breaking.

In the process of HF, the vertical and horizontal fracture radii are

generally fast at the initial stage and slow during the rest of time (Fig. 15(b)). The fracture radius grows rapidly owing to the intersection of hydraulic fractures and random cracks, and the crack tips continuously expand in the early stage. However, the hydraulic fractures are mainly formed near the injection hole in the later stage, so the growth of the crack radius is slow. As with the orthogonal coal model, the SRM model greatly increases the porosity growth rate, which is approximately 17% (Fig. 15(a)) after HF is finished. As a consequence, it can be seen from these results that stochastic structural planes in coal will contribute to the formation of a complex fracture network and that it will also increase the porosity of the coal in fractured zones, thus indirectly improving the permeability of the coal.

5. The effect of natural fracture patterns on HF propagation

When the HF extends to the natural fracture, it is found that the hydraulic fracture bifurcates, and a network of complex fractures forms (Warpinski and Teufel, 1987). We also observe this phenomenon from the numerical simulation results of HF on the five types of coal rock mass models as mentioned previously. The three kinds of fracture modes observed in the field of mines (Wu et al. (2006)) should be affected mostly by the natural fracture distribution.

The effect of natural fractures on hydraulic fractures can be divided into two stages. In the first stage, the hydraulic fracture tip reaches the natural fracture, and there are two possibilities—the natural fracture captures the hydraulic fracture, or the hydraulic fracture crosses the natural fracture. In the second stage, it is possible that the hydraulic fracture propagates along or crosses the natural fracture, or both propagating and crossing occur (Gu et al., 2011).

Based on the simulation results of HF (see Fig. 16), three patterns for the effect of natural fractures on the propagation of hydraulic fractures can be categorized.

Capturing: As a hydraulic fracture reaches a natural joint plane, shear slip may occur on the joint plane, or the hydraulic fracture is captured by the joint plane, which prevents the propagation of the hydraulic fracture. Then, the fluid in hydraulic fracture flows into the joint plane, which is expected to become a part of the hydraulic fracture network, the path of which is thus changed and continuously propagates along the joint plane.

Crossing: The hydraulic fracture crosses the joint plane and extends along the original path with the natural joint plane remaining closed.

Compound: The hydraulic fracture not only crosses the joint plane but also propagates along joint plane into which the fluid flows.

As one can see, the simulation results can prove the correctness of model provided by Gu et al. (2011).

By tracking and studying local hydraulic fractures, it can be speculated that in the expansion process of HF, significant stress is induced in the vicinity of the crack tip. Under the action of this stress, tension or shear failure is likely to occur; an originally closed crack is expanded and continuously propagates along the joint by the follow-up high-pressure fluid.

6. Conclusions

According to the research of fracturing regularity on five types of coal rock mass models, it is found that in the HF simulation of intact coal, a relatively complete and continuous crack is eventually formed, and the crack propagation orientation is parallel to the direction of the maximum principal stress. In addition, the existence of joint surface has an induced effect on the propagation of the crack. In the HF crack propagation process, a large induced stress is generated near the crack tip. The natural fractures are likely to be damaged because of this large induced stress, so the subsequent injection of high-pressure fluid leads the fractures to propagate further.

The fracture radius, cumulative crack number, and growth rate of porosity in the HF models mainly increase in a linear or polynomial manner with the increase of injection time. The existence of natural fractures will contribute to the formation of a complex fracture network and increase the porosity of coal in the fractured region, thus indirectly improving the permeability of the coal. Based on the results of numerical simulation, three patterns of crack propagation of HF affected by the natural fractures can be categorized—capturing type, crossing type, and compound type. Further analysis of the relationship between the induced stress at the crack tip and the mechanical properties of the front discontinuity is needed for the discrimination of crack propagation patterns in the future.

Acknowledgments

This study was funded by the National Natural Science Foundation of China (NSFC) under the Contract no. 51428902 and 51304237, by State Key Laboratory of Coal Resources and Safe Mining under the Contract no. SKLCSRSM14KFB06.

References

- Adachi, J., Siebrits, E., Peirce, A., Desroches, J., 2007. Computer simulation of hydraulic fractures. *Int. J. Rock Mech. Min. Sci.* 44, 739–757.
- Al-Busaidi, A., Hazzard, J.F., Young, R.P., 2005. Distinct element modeling of hydraulically fractured Lac du Bonnet granite. *J. Geophys. Res. Solid Earth* 110 (B6), 1–14, (B06302).
- Camones, L.A.M., Vargas, E.D.A., Jr., de Figueiredo, R.P., Velloso, R.Q., 2013. Application of the discrete element method for modeling of rock crack propagation and coalescence in the step-path failure mechanism. *Eng. Geol.* 153, 80–94.
- Chang, H., 2004. Hydraulic Fracturing in Particulate Materials (Ph.D. thesis). Georgia Institute of Technology, Atlanta, Georgia, USA.
- Cipolla, C.L., Wright, C.A., 2000. Diagnostic Techniques to Understand Hydraulic Fracturing: What? Why? and How? SPE paper 59735 presented at the 2000 SPE/CERI GasTechnology Symposium. Calgary, Alberta Canada. pp. 1–13.
- Du, C., 2008. Study on Theoretics of Hydraulic Fracturing in Coal Bed and its Application (Ph.D. thesis). China University of Mining and Technology, Xuzhou, China.
- Duan, K., Kwok, C.Y., 2015. Discrete element modeling of anisotropic rock under Brazilian test conditions. *Int. J. Rock Mech. Min. Sci.* 78, 46–56.
- Fan, T., Zhang, G., Cui, J., 2014. The impact of cleats on hydraulic fracture initiation and propagation in coal seams. *Pet. Sci.* 11 (4), 532–539.
- Grasselli, G., Lisjak, A., Mahabadi, O.K., Tatone, B.S.A., 2014. Influence of pre-existing discontinuities and bedding planes on hydraulic fracturing initiation. *Eur. J. Environ. Civ. Eng.* 19, 580–597.
- Gu, H., Weng, X., Lund, J.B., Mack, M.G., Ganguly, U., Suarez-Rivera, R., 2011. Hydraulic fracture crossing natural fracture at non-orthogonal angles, a criterion, its validation and applications. Paper SPE 139984 Presented at the SPE Hydraulic Fracturing Technology Conference, Texas, TW, pp. 20–26.
- Gui, N., Fan, J.R., Chen, S., 2010. Numerical study of particle–particle collision in swirling jets: a DEM–DNS coupling simulation. *Chem. Eng. Sci.* 65 (10), 3268–3278.
- Han, Y., Cundall, P.A., 2013. LBM–DEM modeling of fluid–solid interaction in porous media. *Int. J. Numer. Anal. Methods Geomech.* 37 (10), 1391–1407.
- Han, Y., Damjanac, B., Nagel, N., 2012. A microscopic numerical system for modeling interaction between natural fractures and hydraulic fracturing. In: Proceedings of the 46th US Rock Mechanics/Geomechanics Symposium, Chicago, IL.
- Hou, B., Chen, M., Wang, Z., Yuan, J., Liu, M., 2013. Hydraulic fracture initiation theory for a horizontal well in a coal seam. *Pet. Sci.* 10 (2), 219–225.
- Huang, B., 2009. Research on Theory and Application of Hydraulic Fracture Weakening for Coal-rock Mass (Ph.D. thesis). China University of Mining and Technology, Xuzhou, China.
- Hubbert, K.M., Willis, D.G., 1957. Mechanics of hydraulic fracturing. *J. Pet. Trans.* 210, 153–166.
- Itasca Consulting Group Inc., 2010. PFC2D-Particle Flow Code in Two Dimensions. Ver. 4.0 User's Manual. ICG, Minneapolis.
- Li, D.Q., Zhang, S.C., Zhang, S.A., 2014. Experimental and numerical simulation study on fracturing through interlayer to coal seam. *J. Nat. Gas Sci. Eng.* 21, 386–396.
- Li, H., Wong, L.N.Y., 2012. Influence of flaw inclination angle and loading condition on crack initiation and propagation. *Int. J. Solids Struct.* 49 (18), 2482–2499.
- Li, L.D., Zhang, S.C., Geng, M., 2010. CBM reservoir hydraulic fracture propagation rule. *Nat. Gas Ind.* 30 (2), 72e74.
- Li, W., Soliman, M., Han, Y., 2016. Microscopic numerical modeling of Thermo-Hydro-Mechanical mechanisms in fluid injection process in unconsolidated formation. *J. Pet. Sci. Eng.* 146, 959–970.
- Mas Ivars, D., Potyondy, D.O., Pierce, M., Cundall, P.A., 2008. The Smooth-Joint Contact Model (Abstract). In: Proceedings of 8th World Congress on Computational Mechanics/5th European Congress on Computational Methods of Applied Science & Engineering, Venice, Italy. Paper No. a2735. B.A. Schrefler and U. Perego, Eds. Barcelona: International Center for Numerical Methods in Engineering (CIMME).

- Mas Ivars, D., Pierce, M.E., Darcel, C., Reyes-Montes, J., Potyondy, D.O., Young, R.P., Cundall, P.A., 2011. The synthetic rock mass approach for jointed rock mass modelling. *J. Int. J. Rock Mech. Min. Sci.* 48 (2), 219–244.
- McLennan, J., Tran, D., Zhao, N., Thakur, S., Deo, M., Gil, I., Damjanac, B., 2010. Modeling fluid invasion and hydraulic fracture propagation in naturally fractured rock: a three-dimensional approach. In: *Proceedings of the Presented at International Symposium and Exhibition on Formation Damage Control, Lafayette, LA*, pp. 1–13.
- Papanastasiou, P.C., 1997. A coupled elastoplastic hydraulic fracturing model. *Int. J. Rock Mech. Min. Sci.* 34, 240–241.
- Pierce, M.E., Fairhurst, C., 2012. “Synthetic Rock Mass Applications in Mass Mining”. In: *Harmonising Rock Engineering and the Environment (Proc. 12th ISRM Int. Congress, Beijing, China, October 2011)*, pp. 109–114, Q. Qian and Y. Zhou, eds., ISBN 978-0-415-80444-8, London: Taylor & Francis Group (2012).
- Potyondy, D.O., 2012. The Bonded-Particle Model—a Tool for Rock Mechanics Research and Application: Current Trends and Future Directions. Keynote paper in *The Present and Future of Rock Engineering (In: Proceedings of the 7th Asian Rock Mechanics Symposium-ARMS7)*, Seoul, Korea.
- Potyondy, D.O., Cundall, P.A., 2004. A bonded-particle model for rock. *Int. J. Rock Mech. Min. Sci.* 41 (8), 1329–1364.
- Robinson, M., Ramaioli, M., Luding, S., 2014. Fluid–particle flow simulations using two-way-coupled mesoscale SPH–DEM and validation. *Int. J. Multiph. Flow* 59, 121–134.
- Shan, X.J., Zhang, S.C., Li, A.Q., 2005. Hydraulic fracture propagation rules analysis for coalbed methane well. *Nat. Gas Ind.* 25 (1), 130e132.
- Shimizu, H., 2010. Distinct element modeling for fundamental rock fracturing and application to hydraulic fracturing (Ph.D. thesis). Kyoto University, Kyoto, Japan.
- Shimizu, H., Murata, S., Ishida, T., 2011. The distinct element analysis for hydraulic fracturing in hard rock considering fluid viscosity and particle size distribution. *Int. J. Rock Mech. Min. Sci.* 48, 712–727.
- Vychtil, J., Horii, H., 1998. Micromechanics-based continuum model for hydraulic fracturing of jointed rock masses during HDR stimulation. *Mech. Mater.* 28, 123–135.
- Wang, J.G., Zhang, Y., Liu, J.S., Zhang, B.Y., 2010. Numerical simulation of geofluid focusing and penetration due to hydraulic fracture. *J. Geochem. Explor.* 106, 211–218.
- Wang, T., Xu, D., Elsworth, D., Zhou, W., 2016. Distinct element modeling of strength variation in jointed rock masses under uniaxial compression. *Geomech. Geophys. Geo-Energy Geo-Resour.* 2 (1), 11–24.
- Wang, T., Zhou, W., Chen, J., Xiao, X., Li, Y., Zhao, X., 2014. Simulation of hydraulic fracturing using particle flow method and application in a coal mine. *Int. J. Coal Geol.* 121, 1–13.
- Wang, Y., Tonon, F., 2009. Modeling Lac du Bonnet granite using a discrete element model. *Int. J. Rock Mech. Min. Sci.* 46 (7), 1124–1135.
- Warpinski, N.R., Teufel, L.W., 1987. Influence of geologic discontinuities on hydraulic fracture propagation (includes associated papers 17011 and 17074). *J. J. Pet. Technol.* 39 (2), 209–220.
- Wright, C.A., Tanigawa, J.J., Mei, S.X., Lei, Z.G., 1995. Enhanced hydraulic fracture technology for a coal seam reservoir in Central China, presented at International Meeting on Petroleum Engineering, Beijing, China, 14e17 November.
- Wu, X., Xi, C., Wang, G., 2006. The mathematic model research of complicated fractures system in coalbed methane wells. *Nat. Gas Ind.* 26 (12), 124–126.
- Yuan, Z., Wang, H., Liu, N., Liu, J., 2012. Simulation study of characteristics of hydraulic fracturing propagation of low permeability coal seam. *Disaster Adv.* 5 (4), 717–720.
- Zhang, F., Nagel, N., Sheibani, F., 2014. Evaluation of Hydraulic Fractures Crossing Natural Fractures at High Angles Using a Hybrid Discrete-Continuum Model. In: *Proceedings of the 48th US Rock Mechanics/ Geomechanics Symposium*. MN, USA, ARMA-14-7540.